Renewable Energy 68 (2014) 752–760

Contents lists available at ScienceDirect

Renewable Energy

journal homepage: www.elsevier.com/locate/renene

Reconsidering the capacity credit of wind power: Application of cumulative prospect theory

Edgar Wilton [a,*], Erik Delarue [b], William D'haeseleer [b], Wilfried van Sark [a]

[a] Copernicus Institute of Sustainable Development and Innovation, Utrecht University, Heidelberglaan 2, 3584 CS Utrecht, The Netherlands
[b] University of Leuven (KU Leuven) Energy Institute, TME Branch (Applied Mechanics and Energy Conversion), Celestijnenlaan 300A, Box 2421/B-3001 Leuven, Belgium

ARTICLE INFO

Article history:
Received 5 September 2013
Accepted 28 February 2014
Available online 27 March 2014

Keywords:
Capacity credit
Cumulative prospect theory
Variable wind time series analysis
Behavioral energy planning

ABSTRACT

The capacity credit is often erroneously considered to be a time-invariant quantity. A multi-year analysis of the incident wind profile of various potential wind sites uncovered that there exist large differences between annual capacity credit figures. The uniformity of these capacity credit figures is found to decrease with diminishing wind time series interval lengths. In recognition of the resulting uncertainty, decision maker risk propensity toward various capacity credit scenarios was investigated by adopting cumulative prospect theory. The methodology proposed in this paper is an extension of the effective load carrying capability method. It enables the quantitative analysis of the attitudes of decision makers with regard to deviations (gains and losses) from the forecasted capacity credit as a result of the uncertainty of the incident wind profile. Here, gains and losses may not be viewed by decision makers as having equal but opposite effects on the appeal of wind power production. Therefore, it is argued that a decision maker will not have a neutral risk propensity toward changes to the outcome of the capacity credit and will discount increases and decreases of the loss of load expectation according to a non-linear preference. In line with the well-known adagium that losses loom larger than gains the value of the capacity credit is found to be lower than its corresponding least squares forecast.

1. Introduction

Since the adoption of the '20-20-20'goals [1], several EU countries have acknowledged that increasing their use of wind power could significantly aid in lowering their greenhouse gas emissions. However, any successful attempt to transition to a power system with high installed wind capacity levels will need to take into consideration that on occasion there will be periods of little to no wind due to the intermittent nature of this resource. Therefore, in order for a power system to perform its intended function, reliably supplying electricity to the end-consumer, the magnitude of the contribution of wind power generation to the reliability of the power system needs to be determined.

Next to the need for load-balancing during average-load days, a stable power system must also possess enough installed reserve capacity to deal with unexpected contingencies. The latter is referred to as a power system's adequacy. Adequacy determines the degree to which a power system has sufficient generation facilities to satisfy consumer demand. This is not to be confused with the security of a power system, which evaluates how well a system is able to handle local or widespread disturbances, such as the loss of one (or several) generating units [2].

A well-documented method for assessing the adequacy of a wind power generation system is by determining its capacity credit (CC) (e.g. Ref. [3]). This can be defined as *the amount of additional load a system can serve as a result of the addition of a generator without altering the existing reliability level* [4].[1]

The investigation of the value of wind power and the effects of the time series length on the CC performed in this paper was prompted by a growing awareness that sudden extended low wind periods may have severe consequences for the system reliability of power systems with a high wind power penetration. For instance, it is stated in Leahy and Foley [6] that it is likely that the CC is sensitive to the occurrence and frequency of extreme weather events. Furthermore, in Gilotte [7] it is recognized that the CC does not take

* Corresponding author.
E-mail address: edgar.wilton@gmail.com (E. Wilton).

[1] It should be noted that the CC can also be defined as the amount of *conventional power generation capacity reduction* that can be achieved without affecting the loss of load probability (e.g. Ref. [5]).

http://dx.doi.org/10.1016/j.renene.2014.02.051
0960-1481/

into consideration that the increased power outage probability, resulting from extended periods with low wind availability, may not be compensated by a reduction of the power outage probability during periods with relatively abundant wind availability.[2] In other words, the typical decision maker may value equal magnitudes relative to a reference point differently depending on whether they are categorized as 'gains' or 'losses' relative to some expectation level. Consequently, it can be argued that the CC should be valued according to a methodology that incorporates this reference dependence. Therefore, in this paper the use of cumulative prospect theory (CPT) is proposed for the first time as an extension of CC analysis.

CPT is a fully empirical descriptive decision theory that derives the value of an uncertain prospect by means of a frame, a value function and a non-linear decision weighting function. It is rooted in behavioral psychology and has demonstrated to possess sufficient explanatory power for use in actual decision making problems [8]. It is argued in this paper that it could also be used to address the issue of properly valuing the occurrence of deviant weather patterns. This is especially true when the time series interval (TSI) on which the CC is evaluated is reduced to a length of several weeks. The reduction of the time series interval reveals the underlying variability of the incident wind profile. Furthermore, this segregation of the wind time series enables the identification of extended low wind periods that would otherwise have gone unnoticed as a result of the inconsequentiality of a bi-/triweekly time frame on the typical measurement interval of one year.

This paper begins with a brief literature review of the utilized capacity credit methodology, an investigation of the use of CPT in engineering literature thus far and a description of its foremost characteristics. Subsequently, the proposed methodology is applied to a case study where a high installed wind capacity is added to the existing thermal generation capacity of the Netherlands. Afterward, the results are presented, discussed and the main findings are summarized in the conclusion.

2. Literature review

2.1. Capacity credit

The International Energy Agency (IEA) considers computation of the effective load carrying capability (ELCC) of a power system, by means of a loss of load probability (LOLP) analysis using chronological load demand patterns, to be the most rigorous methodology available for estimating the CC [9]. This claim is backed by the Institute of Electrical and Electronics Engineers (IEEE), which also appears to favor the ELCC method for assessing the CC [4].

The ELCC method analyzes the capacity credit from an incremental load addition standpoint. Here, it is assumed that thermal generators are still relatively abundant and that the overall system reliability can be modeled by means of their rated power output and forced outage rate (FOR) alone.

Over sufficiently large time intervals, the FOR can also be approximated by dividing the forced outage hours by the sum of the in-service hours and forced outage hours [2]. The FOR and rated capacity values of the thermal generator set are subsequently used to determine the capacity outage probability table (COPT). The cumulative probability values corresponding to each of the various possible available generation states can then be used to determine the LOLP, which is given by

$$\mathrm{LOLP}_t = P\left(\sum_{g=1}^{G} C_{g,t} < L_t\right) \tag{1}$$

where $C_{g,t}$ represents the rated capacity of generator g, during hour t and L_t equals the load demand during hour t. As discussed by Kahn [10], when determining the LOLP values over a certain time frame, the LOLP can be used to derive the expected power outage length over that time frame. The acquired variable is the loss of load expectation (LOLE), which can be defined for any particular time interval, given that it is measurable on the unit scale of the LOLP (in this case hours t), as follows

$$\mathrm{LOLE} = \sum_{t=1}^{T} \mathrm{LOLP}_t \tag{2}$$

Here, T denotes the TSI length. Furthermore, it should be noted that a common planning objective is the '1-day-in-10-years' reliability criterion, which implies a system reliability of approximately 99.97% [10].

Garver [11] defined the ELCC as the magnitude of the incremental lo ad addition ΔL that can be supported by a system at the initial LOLE following a certain capacity addition ΔC. An implicit definition of the ELCC can then be given by stating that the initial LOLE, with a given incremental load addition, may not exceed a predetermined power system reliability criterion (LOLE_R). The corresponding value of the ELCC can subsequently be ascertained by iteratively determining the maximum incremental load addition ΔL:

$$\max_{\Delta L \in \mathbb{R}^+} \Delta L \qquad \text{(Objective function)}$$

$$\sum_{t=1}^{T} P\left(\sum_{g=1}^{G} C_{g,t} + \Delta C < L_t + \Delta L\right) \le \mathrm{LOLE}_R \qquad \text{(Reliability constraint)}$$

This approach, although ideal for classical thermal generation stations, does not allow for the adequate analysis of systems with intermittent power sources, such as wind turbines. This is due to the fact that for wind turbines the capacity and FOR are more dependent on the availability of wind resources than on mechanical constraints. Therefore, in order to accurately incorporate wind generation, the time series of the wind power plant output is treated as *negative* load demand considering that all the load that is served by wind power does not have to be supplied by thermal generators. The difference between the ELCC with and without the addition of wind power is considered as the CC of a certain installed wind capacity.

2.2. Cumulative prospect theory

It has been noted that the study of wind power consists of two relevant time horizons [12]. These are the short-term, which includes the decisions pertaining to the optimal wind energy offerings and conjoining levels of operational backup, and the long-term, which foresee the capacity backup investments that will be necessary to ensure the continued adequacy of the power system. Risk assessment is already extensively featured in short-term modeling practices. That is, several methodologies have been developed that either mitigate some form of risk associated with the profits realized from wind power generation [13,14] or allow the attitudes of dispatchers with regard to risk and cost to be included in dispatch and unit-commitment models [15,16].

With regards to the long-term, it has been argued in Gilotte [7] that the LOLE, being an expectation, is risk-neutral by nature. Considering that decision makers have been known to be

[2] Moreover, the massive overcapacity during extended periods of wind abundance places additional stress on the system, potentially *increasing* the LOLP.

particularly risk averse regarding the stability of critical infrastructure such as the power grid, this assumption does not necessarily correspond with intuition (e.g. Ref. [17]). Therefore, it is argued by Gilotte that a decision maker will not weigh the benefits of a reduced LOLP during a benign winter on an equal footing with an increased LOLP during a harsh winter.

To incorporate the discomfort of the increased outage probability during harsh winters in the CC methodology, Gilotte proposed the 'risk-corrected capacity credit' (RCC) which computes the LOLE of the 5% worst wind years by means of hourly load demand figures and wind speed estimates. However, this approach entails increasing the energy security at the cost of the energy affordability. In other words, it is not necessarily welfare maximizing to mitigate risk until the system reliability probability borders on certainty. Nevertheless, it is rightfully claimed by Gilotte [7] that the evaluation of the CC could benefit from reflecting upon the risk propensity of the decision maker given that the LOLP is directly tied into the concept of energy adequacy.

It is proposed in this paper that, in a similar fashion to energy security modeling, energy adequacy models, such as the CC methodology, could stand to benefit from a fundamental understanding of how risk acceptance attitudes affect choices. One possible application could be optimizing investments in backup capacity for intermittent renewable resources in correspondence with the risk propensity of a typical utility company. Indeed, it was found by Wu and Huang [18] that the level of investment in backup capacity (total generation costs) is inversely proportional to the CC. It should be noted that the overall effect on the total generation costs was small, however this may be a consequence of the limited share of wind power in the total installed capacity used in the case study.

CPT has the potential to align decisions with the decision maker's risk propensity. This has already been recognized in the risk assessment of low-probability high consequence events in civil engineering [19,20]. Indeed, in Cha and Ellingwood [19] the inclusion of risk aversion had a notable strengthening effect on optimal level of seismic design features in civil infrastructure exposed to low-probability events with severe consequences, such as earthquakes, hurricanes or floods.

The foremost advantage of CPT is that it presents a theoretically sound framework to model a decision maker's subjective probability perceptions in a tractable and intuitive manner. Moreover, CPT exhibits decent empirical characteristics [21]. However, as noted by Cha and Ellington [19], any practical evaluation by means of CPT requires extensive information regarding the decision maker's preferences. These include the perception of the likelihood of events as well as their perceived magnitude. Information on the perceived probability of a loss of load event and its perceived magnitude could be difficult to ascertain, as would be the case for all 'preferences' related to rare natural or man-made hazards. However, despite the additional complexities that come with CPT-based decision models, it is recognized by several authors that risk aversion is a real phenomenon in many engineering problems with low-probability, high consequence events and that CPT offers a unique flexibility in this regard [19,20,22].

The prospect of a certain installed wind capacity $(x_1,p_1\ldots;x_n,p_n)$ is comprised of a range of CC values x_i, the number of which depends on the TSI length, and their corresponding probabilities of occurrence p_i, where $\sum_{i=1}^{n} p_i = 1$.

Prospect theory distinguishes between two phases: the editing phase, which consists of a preliminary analysis of the prospect, and the evaluation phase in which the overall value of the edited prospect V is determined [23]. During the editing phase, the data is reorganized and reformulated with the intent of simplifying the subsequent evaluation. In the evaluation phase the value V is expressed in terms of two scales: the value function $v(x_i)$, which relates to the subjective value of an uncertain outcome, and the decision weights π_i^+ and π_i^-, which involve the perceptual likelihood of a certain probability. During the editing phase the prospect $p_1x_1\ldots p_nx_n$ is reorganized to conform to $x_1 \geq \ldots \geq x_k \geq 0 \geq x_{k+1} \geq \ldots \geq x_n$. Here x_1, and x_n represent the best and worst CC outcomes, occurring with probabilities p_1 and p_n, respectively. In line with Tversky and Kahneman [21], the value V of a prospect in CPT is given as follows

$$V = V^+ + V^- = \sum_{i=1}^{k} \pi_i^+ v(x_i) + \sum_{i=k+1}^{n} \pi_i^- v(x_i) \tag{3}$$

where π^+ and π^- represent the non-linear weighting functions of the gains and losses, respectively, and $v(x)$ gives the non-linear value function. Combined, these subjective parameters capture the preferences of the decision maker regarding the CC gains and losses relative to the frame. This can be understood as that the carriers of value are changes in relative welfare instead of final states [23].

In line with Tversky and Kahneman [21], the value function $v(x)$ can be defined as

$$v(x) = \begin{cases} x^g & x \geq 0 \\ -\lambda(-x)^l & x < 0 \end{cases} \tag{4}$$

where g, l and λ, of which the latter represents the loss aversion factor, are empirically determined parameters. It should be noted that based upon the hypotheses of loss aversion and diminishing sensitivity that $g < l < 1$. The corresponding values for g and l were taken to equal 0.88 and 0.92 in line with Abdellaoui [24]. Furthermore, the loss aversion factor λ is usually taken to equal 2.25; the median value for λ found by Tversky and Kahneman (1992) [21].

The value function is depicted in Fig. 1. Here, the parameters were symmetrically varied in order to display their effect on the overall shape of the functions.

CPT weights the value of an uncertain outcome by a decision weight $w(p)$, a monotonically increasing function of p. It should be noted that $w(p)$ is not a probability. As stated by Tversky and Kahneman 'the decision weights are a measure of the impact of events on the desirability of a prospect and not merely a perceived likelihood' of said events [23]. The non-linear rank-dependent decision weight for gains are given by the following formulas [21]

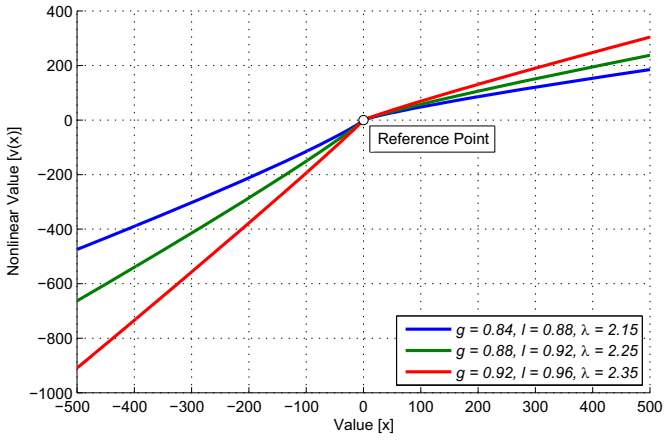

Fig. 1. A value function utilizing various sets of parameter values. The parameter set designated by the green curve is in common use. (For interpretation of the references to color in this figure legend, the reader is referred to the web version of this article.)

$$\pi_i^+ = w^+\left(\sum_{j=i}^{n} p_j\right) - w^+\left(\sum_{j=i+1}^{n} p_j\right) \tag{5}$$

$$\pi_i^- = w^-\left(\sum_{j=1}^{i} p_j\right) - w^-\left(\sum_{j=1}^{i-1} p_j\right) \tag{6}$$

where w^+ and w^- are referred to as the non-linear weighting functions, which can be viewed as non-linear transformations of probabilities into decision weights. First introduced in Refs. [23], they explain the common-ratio effect; the constant ratio that seemed to exist between actual and perceived probabilities. As noted by Goda and Hong [20] the weighting function for the gains takes the form of the exceedance probability while the weighting function for losses takes the form of the cumulative probability.

Several weighting functions have been developed over the years (e.g. Refs. [21,25,26]). Of these, the compound invariance family proposed by Prelec [26] has been praised for its analytical tractability, its suitability for very small and very large probabilities, but foremost for its firm behavioral foundation. The compound invariance family for gains and losses is given by

$$w^+\left(\sum_{j=i}^{n} p_j\right) = \exp\left(-\beta^+\left(-\ln\left(\sum_{j=i}^{n} p_j\right)\right)^{\alpha}\right) \tag{7}$$

and

$$w^-\left(\sum_{j=-m}^{i} p_j\right) = \exp\left(-\beta^-\left(-\ln\left(\sum_{j=-m}^{i} p_j\right)\right)^{\alpha}\right) \tag{8}$$

where β^+, β^- and α are the model parameters that determine the concavity and convexity of the inverse S-shaped weighting function that is characteristic for the fourfold pattern of risk attitudes. The latter is considered to be one of the most distinctive implications of prospect theory [21]. It dictates that a typical decision maker displays risk-seeking behavior for low-probability gains and high-probability losses, while simultaneously being risk averse for high-probability gains and low-probability losses. This behavior can be refined from Prelec's function by separately interpreting the compound invariance functions for gains and losses. Considering that the definition of what is considered a gain or a loss is rooted in the choice of the frame, findings for the loss-rank can be translated into findings for the gain-rank and vice versa (i.e. β^- equals β^+). It is suggested by Wakker [22] that good parameter choices for β and α are 1.0467 and 0.65. The aforementioned and several other parameter choices for the weighting function can be found in Fig. 2.

Finally, it should be noted that there is no empirical evidence to support the parameter assumptions for either the value functions or the weighting functions. It is by no means implied that they represent the actual risk propensity of the typical decision maker toward loss of load events. That is, for the purpose of illustrating the proposed methodology commonly encountered parameter choices were used. Furthermore, accurate determination of the parameters involved is left for future research.

3. Case study

The wind data used in this paper were acquired from public databases of the KNMI, the Royal Netherlands Meteorological Institute [27]. The potential wind time series runs from January 1st 2001 to December 31st 2012. Considering that the potential wind data of various years has to be matched with the load demand time series of 2011, the length of the potential wind data in leap years was reduced to 8760 h. In order to preserve the internal consistency of the wind time series, all corrections were made at the end of the year. That is, for every year that contained a 29th of February the wind data of the 31st of December was removed as compensation. A rough approximation of the wind speed at hub height can be acquired by means of the logarithmic law. This is a simplification of the log-linear law that assumes neutral atmospheric stability [28]:

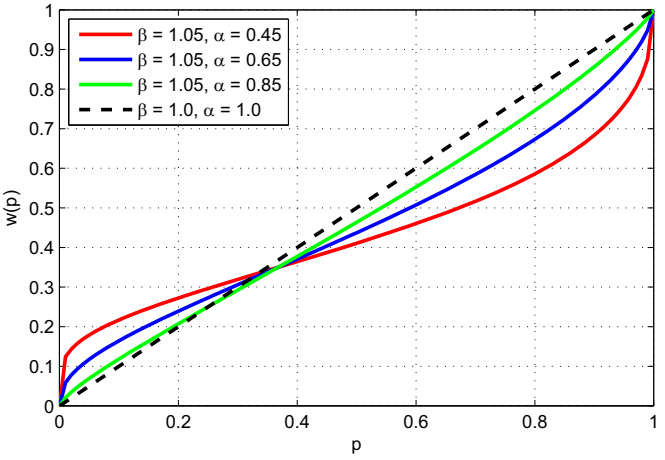

Fig. 2. Several variants of Prelec's compound invariance function [26] representing a variety of risk attitudes.

$$v_2 = v_1\frac{\ln(z_2/z_0)}{\ln(z_1/z_0)} \tag{9}$$

Here v_1, represents the wind speed [m/s] at measurement height z_1 [m] v_2, [m/s] equals the wind speed at hub height z_2 [m] and z_0 corresponds to the roughness length [m], which is taken to equal 0.03 m. It should be noted that the resulting approximation of the wind speed at hub height will most likely not result in wind speed profiles of the highest possible accuracy. However, the purpose of this paper is not to obtain accurate evaluations of the wind speed potential. Subsequently, the power output of a wind turbine can be determined by means of the well-known expression

$$P = \frac{1}{2}C_p\rho A v_2^3 \tag{10}$$

which can be found in any typical wind-engineering textbook (e.g. Ref. [29]). In this equation C_p, represents the turbine power coefficient [−], ρ is the air density [kg/m^3], A equals the area swept by the rotor [m^2] and v_2 is the wind speed at hub height [m/s] C_p values were acquired from the technical specifications of the Enercon E-126 [30]; the chosen reference turbine which has a rated capacity of 7.58 MW.

The installed wind power capacity was added in increments of 50 E−126 turbines (379 MW) equally distributed across the 10 anemological zones designated by the meteorological stations shown in Fig. 3. The selection of these stations was influenced by the original inquiry made into the CC of wind power in the Netherlands performed by van Wijk et al. [5]. Furthermore, the installed capacity cap was set to 1000 turbines for a total of 7580 MW of rated capacity.

An inventory of the thermal generation capacity in the Netherlands (≥ 100 MWe) was acquired from TenneT [32]. In addition, several generators were added with rated capacities below this benchmark. Consequently, the thermal generator data

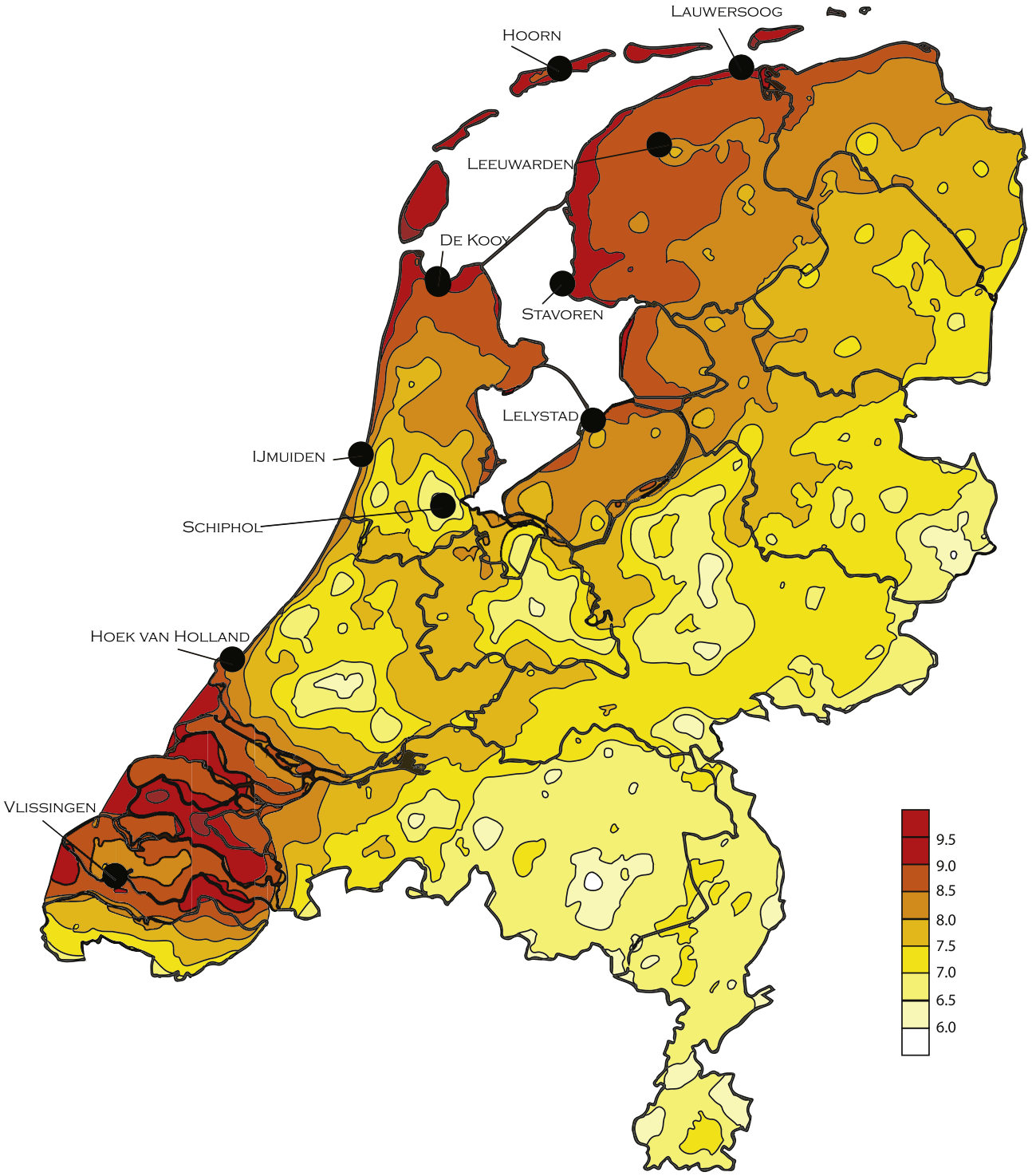

Fig. 3. A wind map of the Netherlands displaying average wind speeds, ranging from below 6 m/s for the vale yellow areas up to above 9.5 m/s for the bright red areas [31]. The black dots indicate the locations of the selected meteorological stations. (For interpretation of the references to color in this figure legend, the reader is referred to the web version of this article.)

set is comprised of all thermal generators with an electrical power output in excess of 50 MW in the Netherlands.[3] The corresponding FOR values were approximated by means of annual world average availability data (segregated per station type and power output class) published by the World Energy Council [33]. Depending on the power output size, the FOR was determined to be within the 0.04–0.12 h_{out}/h[4] range for coal-fired power plants and to vary between 0.05 and 0.09 h_{out}/h for conventional gas turbines. It

[3] Courtesy of E.ON and Nuon. This includes all CHP units with an electrical power component of 50 MW or more.

[4] The number of forced outage hours divided by the sum of the in-service hours and forced outage hours.

should be noted that FOR values of the latter result in a slightly overestimated LOLE due to the majority of the gas turbines in the Dutch power system being CCGTs, which typically have higher availability factors than their conventional counterparts.

The CC reference and its corresponding value function V were computed for 219, 438, 730, 2190, 4380, 8760 and 17520-h TSIs (representing biweekly, triweekly, monthly, quarterly, semi-annual, annual and biannual time frames). In order to obtain a reference frame for the CC against which the magnitude of the gains and losses can be derived, a rational polynomial[5] was fitted to the absolute CC and the installed wind capacity. Based on the composition of the CC data set, a first order rational polynomial was deemed to possess sufficient degrees of freedom. The resulting curve was designated as the *capacity credit forecast* (CCF). Following the identification of the magnitude and sign corresponding to each individual data point, a single value V was determined for each installed wind capacity increment. After computing the value V of each set of data points, 20 V-values were acquired per TSI. For consistency purposes, these value points were also fitted with a first order rational polynomial, the result was denoted as the *capacity credit value* (CCV) curve.

The TSI lengths were not chosen arbitrarily. In Leahy and Foley [6] it is stated that from the second week of December 2009 onwards wind conditions on the Irish isle started to deteriorate, with below average wind conditions being reported for the remainder of the month. The period from the 19th to the 30th of December was proclaimed to have been of particular interest. These time frames, roughly three and two weeks in length, respectively, were approximated by taking factorizations of 8760 h. This was done in order to preserve the chronological match between the wind and load demand time series. TSIs of 438 and 219 h in length were deemed to be appropriate approximations. Additionally, the interval lengths in-between the three-week and annual mark, such as a month and a semi-quarter (length of a season), were added for the sake of completeness.

4. Results

4.1. 8760-Hour time series interval

In order to verify the proper functioning of the CC model, the initial TSI was set to equal 8760 h, with the start and endpoints set to January 1st and December 31st respectively. This approach, in which the beginning and ending of a calender year is used to define the parameters of the TSI is often encountered in contemporary CC studies (e.g. Refs. [34,35]).

Inspection of Fig. 4 verifies that the CCF displays the same diminishing marginal returns trend for increasing levels of installed wind capacity that is encountered in similar CC studies (e.g. TradeWind [34]). Furthermore, it should be noted that the CCV is lower than the CCF, which can be attributed to loss aversion.

The decreasing marginal returns for increasing installed wind capacity levels are an inherent consequence of the intermittent nature of wind power. When there is a relatively low dependence on wind power, a sudden calm will have a minimal impact on overall grid stability. However, at high installed wind capacity levels, any calm could remove a significant share of the wind power capacity from the grid, thereby lowering the CC. Other factors which are known to influence the CC are: the average wind speed, the overall system reliability, the wind farm capacity factor, the correlation between demand and wind, the correlation of the wind speeds of the various wind farm sites (geographical spread) and the degree of wind power exchange between systems [36].

[5] A ratio of two polynomial functions.

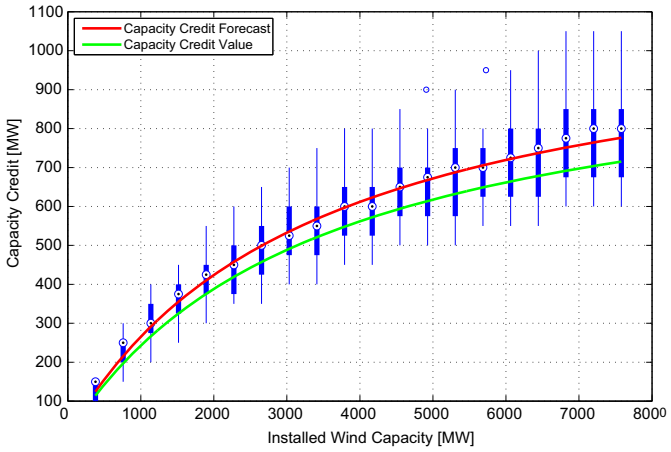

Fig. 4. The CC data (represented by means of box plots) and the CCF and CCV curves of 8760-h chronological wind time series samples. For each box, the central mark is the median, the edges of the box are the 25th and 75th percentiles, the interquartile range extends 1.5 times the difference between the aforementioned percentiles in each direction and outliers are plotted individually.

4.2. 438-Hour time series interval

As a result of critical role the three-week interval plays in the events discussed in Leahy and Foley [6], it was given special consideration in this paper. It should be noted that, for the purpose of illustrating the effects of CPT and variable time series analysis on the CC, the 219-h TSI could also have sufficed. However, due to ulterior considerations, discussed further in Section 5, the 438-h TSI was considered preferential. The corresponding CCF and CCV curves are shown in Fig. 5.

Firstly, it should be noted that, as a result of the increased wind time series resolution, the CC sample size has increased from 12 to 240 intervals. The enlargement of the sample size correspondingly increases the number of intermittent outcomes and the visibility of the extrema (resulting in a different scaling of the y-axis). This can be inferred from the increase of the interquartile ranges and the number of outliers found in Fig. 5. Secondly, Fig. 5 indicates that, similar to the 8760-h interval, the application of CPT results in the

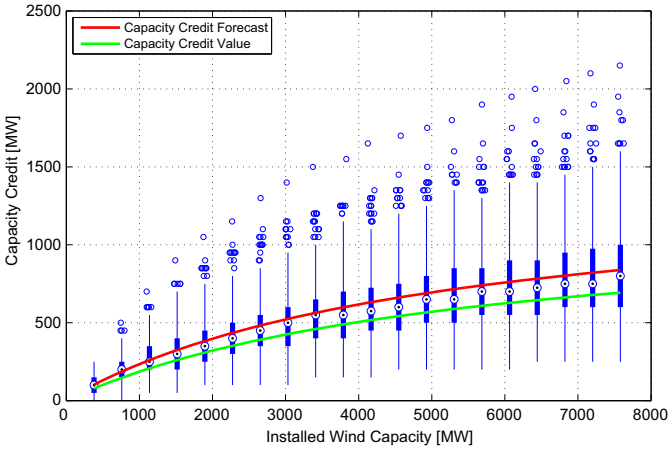

Fig. 5. The CC data (represented by means of box plots) and the CCF and CCV curves of a 438-h chronological wind time series samples.

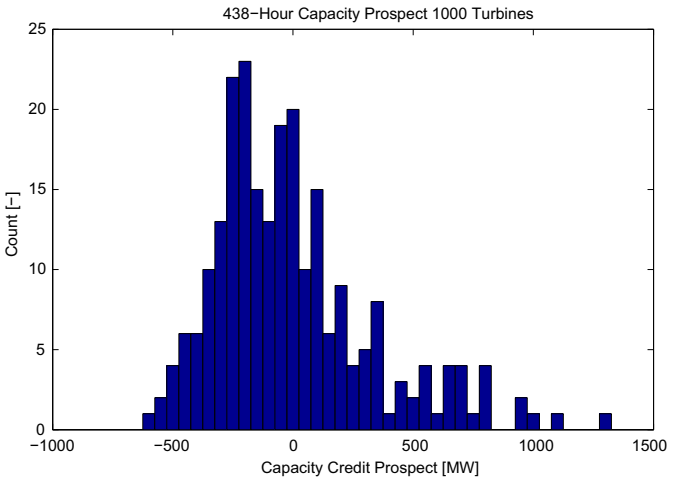

Fig. 6. Histograms displaying the variation in capacity credit prospects for 1000 Enercon E−126 turbines over a chronological TSI of 438 h.

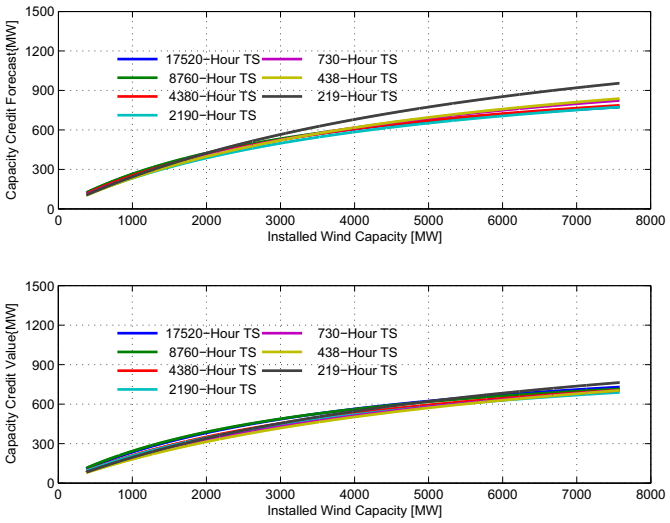

Fig. 7. Comparison of the CCFs (top) and CCVs (bottom) of the various TSIs.

CCV being below the CCF for the entire installed wind capacity range (losses loom larger than gains).

A remark can be made regarding the lower bound of the absolute capacity credit values. As can be visually verified from Fig. 5 extended periods of low wind potential, along the lines of Leahy and Foley [6], were encountered in the data set under investigation. The minimum and maximum CC figures for an installed wind capacity of 7580 MW were found to equal 250 MW and 2150 MW, respectively. Fig. 6 displays these values relative to the frame with their corresponding likelihood. It should be noted that in addition to negative deviations, positive deviations from the CCF were also found to be quite common.

A further inspection of these deviations leads to the realization that although the maximum positive deviations are larger in magnitude, negative deviations are generally more prevalent than their positive counterparts. It can be concluded from Fig. 6 that, at the highest installed wind capacity level, deviations from the frame can be as high as +1300 MW and −600 MW. This implies that any power grid relying on high installed wind capacity levels will have to be able to cope with the occasional forecast deviation, ranging from the addition of a state of the art nuclear power plant to the loss of a typical coal-fired power plant.

5. Discussion

5.1. Forecast and value

Hitherto, the CCF and CCV curves were only displayed relative to one another. However, as discussed in the previous section, the CCF and therefore the CCV are subject to change as the composition of the data set is modified due to TSI variations. Therefore, it is of interest to ascertain the differences in shape when the separate curves are compared amongst each other.

The independent groupings of CCF and CCV curves can be found in Fig. 7. Here, the CCF curves corresponding to the various TSIs appear to differ only marginally from one another. This can be explained by the differences in the data point composition altering the solution to the least squares fitting problem. Furthermore, the CCV is characterized by an even lower differentiation as a result of loss aversion.

It would appear that both the CCF and CCV curves display fairly consistent progression patterns with the only notable exception being formed by the 219-h TSI. Further investigation reveals that both the CCF and CCV curves seem to rise slightly as the TSI length decreases. This is most likely caused by the increased prevalence of (positive) outliers in the shorter TSIs affecting the fitting of the CCF. Consequentially, Fig. 7 suggests that the increased spread of the capacity credit range for shorter TSIs, together with the ensuing appearance of outliers, limits the relevance of the curves fitted to shorter TSI CC datasets.

An additional variable of interest is the relative difference between the CCF and CCV as a function of the installed wind capacity. This is depicted in Fig. 8. It would appear that for all but the 219-h TSI, the relative difference decreases for increasing levels of installed wind capacity. This phenomenon can be explained by the increased relative prevalence of outliers for higher installed wind capacity levels. Furthermore, the similarities between the 219, 2190 and 8760-h intervals should be interpreted as that the annual and quarterly TSIs are less outlier prone, while the biweekly interval is dominated by outliers from a relatively low installed wind capacity onwards which appears to prevent outliers from increasing in relative importance.

The inconsistent behavior of some of the curves near the y-axis can be explained by the relative size of the 50 MW load demand increment being larger for smaller installed wind capacity values. As a result, rounding errors could have a more profound effect on

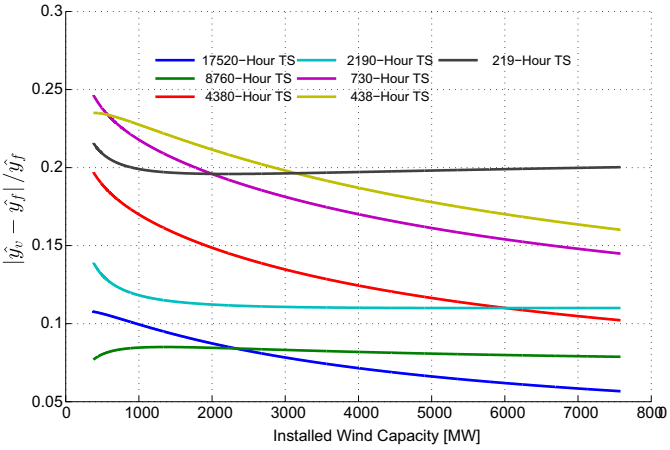

Fig. 8. The relative difference between the CCF and CCV for the various TSIs.

the shape of the curve in the lower installed wind capacity range. Finally, as can be derived from Fig. 8, the relative difference between the CCF and the CCV for higher levels of installed wind capacity ranges from roughly 8–16% (excluding the biannual interval). Moreover, the relative difference tends to increase with decreasing TSI length. This can be attributed to a combination of increased sample size, non-linear preferences and loss aversion.

5.2. Relative capacity credit

As shown in Fig. 9, the CCF of wind power in the Netherlands is located roughly in-between the 27 and 33% for negligible wind capacity penetration levels and can be found to gradually decrease to 10 and 11%, respectively, for a wind capacity penetration above 40%. In line with the European Wind Energy Association (EWE) [36], the wind capacity penetration [%] equals the installed wind capacity [MW] as a percentage of the annual peak load demand [MW].

These findings appear to be in line with the conclusions drawn in the IEA Wind Task 25 [35], where wind power production was found to be capable of contributing up to 40% of its installed capacity for low wind penetration scenarios and down to 5% for high wind power penetration scenarios. This corresponds with the common convention that for negligible wind power penetration levels, the capacity credit resembles the capacity factor of the evaluated wind energy conversion system (e.g. Ref. [9]).

A study conducted by the German Energy Agency resulted in a figure of a similar shape, but with better overall relative capacity credit scores in comparison to the high wind power penetration scenario in this paper [36]. Considering that the German power grid has a similar degree of system security and there is the potential for equivalent wind farm capacity factors, the most likely explanation is a lower degree of wind speed correlation between the various wind sites. This is a consequence of the increased segregation of anemological regions as a result of Germany's comparatively larger land area. The more rapid decay of the Dutch capacity credit indicates that if the Dutch power system were to become highly dependent on wind power for meeting its load demand, large wind capacity outages may not be that uncommon.

Finally, the capacity credit is an uncertain prospect hinging on an inexact knowledge of the composition of the forthcoming wind profile. This uncertainty combined with the possibility of, and our predisposition toward, losses results in a CCV curve that is generally lower than the CCF curve acting as its reference. Additionally, as a result of the annual TSI length chosen in contemporary studies the extended short-term variability of wind power production is systematically underestimated. Therefore not all intermediate states are identified and consequently, as shown in Fig. 9, longer TSIs tend to overstate the value of the wind power resource, by averaging out the deviations in the incident wind profiles.

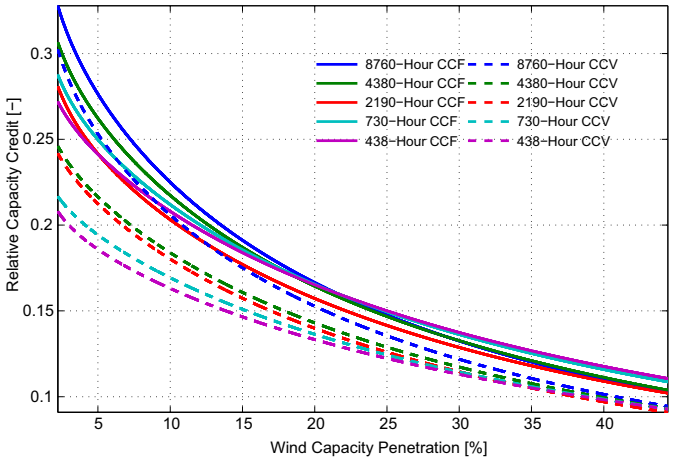

Fig. 9. RCCF and RCCV as a function of the wind power penetration level.

6. Conclusion

In this paper an attempt was made to unify the foremost forecasting mechanism for determining the capacity credit (CC) with modern descriptive decision theory. The latter was specifically created to provide guidelines for valuation under uncertainty. One of the most prominent contemporary descriptive decision theories is cumulative prospect theory (CPT). Considering that the CC of wind power is dependent on an unpredictable incident wind profile, it can be described as an uncertain prospect. Consequently, the profound insights into the nature of value offered by CPT were applied to a range of CC simulations for various wind time series interval lengths.

As a consequence of widespread meteorological events, extended periods of little to no wind could result in the prolonged disuse of wind power generation infrastructure. This could prove to be an inconvenient reality for power systems with a high level of wind power penetration [6]. The resulting strain on the thermal generation capacity increases the outage probability and could lead to extended power outages. However, as a consequence of the length of the time series interval (TSI) considered in conventional capacity credit analysis techniques, such as the effective load carrying capability (ELCC) method, these perturbations are registered as insignificant events. The result is that a lacking overall system reliability in one period is compensated by a system reliability 'excess' in another period.

It can be readily verified that inherent to the concept of expectation is the predisposition of risk-neutrality. As illustrated by Gilotte [7], the outage risk increase resulting from a higher loss of load expectation may not be mentally discounted in a similar fashion as the expected outage risk decrease resulting from a lower loss of load expectation. Although the exact fulfillment of the risk propensity assumed by Gilotte [7] differs from the methodology propagated in this paper, in both cases the existence of a non-linear preferences is implied, one of the main findings of prospect theory [21].

The act of framing revealed that, relative to the reference, the magnitude of the positive CC deviations is much larger than the magnitude of the negative CC deviations, although the latter was found to be far more common. This is in line with the conclusion of a recent study investigating the possibility of a high wind power penetration scenario for the Dutch power system [37]. It was implied here that although the focus usually lies on the risk of generation shortages, the equally important and potentially more pressing matter is what to do with the excess electricity when there is no load demand to meet.

When it comes to the dependability of Dutch wind power generation it should be noted that none of the investigated TSIs gave rise to the result that, for the higher installed capacity scenarios, there are extended periods (down to 219 h) where the CC equals zero. However, the minimum registered CC values during these extended time frames can be considered as negligible nonetheless. As can be expected, the magnitude of the minimum CC figure was found to depend on the chosen TSI.

The relative CC illustrates that a functional small-scale solution does not necessarily have to offer bright mass implementation prospects. Indeed, above a wind capacity penetration of 40% the expected load demand addition will only be roughly 11% of the installed wind capacity. Furthermore, the mass of the CC

distribution is concentrated in the negative domain. Therefore, as a result of loss aversion and overweighting of near impossibilities and near certainties, the corresponding CC value is located in the region of the 10%. It should be noted however that the exact forecast and value figures depend on the length of the TSI and to a certain extent also on its demarcation.

Overall, the main contribution of this paper is twofold. First, an attempt was made to devise a methodology capable of identifying the value of an uncertain wind power generation prospect. Second, the usefulness and limits of long-term wind energy planning by means of decreasing wind TSIs was investigated. For the former it was concluded that, especially for shorter TSIs, the *capacity credit value* is significantly lower than the *capacity credit forecast*, the commonly used guideline. The main body of the CC data points is located in the negative domain relative to the frame. Consequently loss aversion can explain the overall diminishing trend of the capacity credit value. It should be noted however that the parameters describing the risk propensity of the typical decision maker, with regard to the outage risk, were merely approximated. Accurate empirical estimates are yet to be determined. For the latter, it was established that as the TSI length is decreased, the CC spread eventually becomes exceedingly large.

Finally, it should be noted that further analysis is required to assess what would be a reasonable TSI length to evaluate the CC on. Additionally, it should be questioned whether the concept of the CC is still meaningful on TSI lengths of 3 weeks or less considering the wide range of CC figures resulting from the abundant assortment of incident wind profiles.

References

[1] Commission Of The European Communities. Communication from the commission to the European Council and the European Parliament: an Energy Policy for Europe; 2007.
[2] Billinton R, Allen R. Reliability evaluation of power systems. 2nd ed. New York: Plenum Press; 1996.
[3] Voorspools K, D'haeseleer W. An analytical formula for the capacity credit of wind power. Renew Energy 2006;31(1):45–54.
[4] Keane A, Milligan M, Dent C, Hasche B, D'Annunzio C, Dragoon K, et al. Capacity value of wind power. IEEE Trans ower Syst 2011;26(2):564–72.
[5] van Wijk A, Halberg N, Turkenburg W. Capacity credit of wind power in the netherlands. Electr Power Syst Res 1992;23(3):189–200.
[6] Leahy P, Foley A. Wind generation output during cold weather-driven electricity demand peaks in ireland. Energy 2012;39(1):48–53.
[7] Gilotte L. Wind capacity credit: accounting for years of extreme risk. In: Power\Tech, 2011 IEEE Trondheim; 2011. pp. 1–4.
[8] Camerer C. Prospect theory in the wild: evidence from the field. In: Kahneman D, Tversky A, editors. Choices, values, and frames. Cambridge University Press; 2000. pp. 288–300.
[9] Holttinen H, Meibom P, Orths A, Lange B, O'Malley M, Tande J, et al. Impacts of large amounts of wind power on design and operation of power systems, results of IEA collaboration. Wind Energy 2011;14(2):179–92.
[10] Kahn E. Effective load carrying capability of wind generation: Initial results with public data. Electr J 2004;17(10):85–95.
[11] Garver L. Effective load carrying capability of generating units. IEEE Trans Power App Syst 1966;85(8):910–9.
[12] Luickx PJ, Delarue ED, D'haeseleer WD. Considerations on the backup of wind power: operational backup. Appl Energy 2008;85(9):787–99.
[13] Galloway S, Bell G, Burt G, McDonald J, Siewierski T. Managing the risk of trading wind energy in a competitive market. IEE Proc Gener Transm Distrib 2006;153(1):106–14.
[14] Morales J, Conejo A, Perez-Ruiz J. Short-term trading for a wind power producer. IEEE Trans Power Syst 2010;25(1):554–64.
[15] Miranda V, Hang P. Economic dispatch model with fuzzy wind constraints and attitudes of dispatchers. IEEE Trans Power Syst 2005;20(4):2143–5.
[16] Wang L, Singh C. Balancing risk and cost in fuzzy economic dispatch including wind power penetration based on particle swarm optimization. Electr Power Syst Res 2008;78(8):1361–8.
[17] Carreras B, Newman D, Dobson I, Zeidenberg M. The impact of risk-averse operation on the likelihood of extreme events in a simple model of infrastructure. Chaos: Interdiscip J Nonlinear Sci 2009;19(4):1–8.
[18] Wu J-H, Huang Y-H. Electricity portfolio planning model incorporating renewable energy characteristics. Appl Energy 2014;119:278–87.
[19] Cha E, Ellingwood B. Risk-averse decision-making for civil infrastructure exposed to low-probability, high-consequence events. Reliab Eng Syst Saf 2012;104:27–35.
[20] Goda K, Hong H. Application of cumulative prospect theory: Implied seismic design preference. Struct Saf 2008;30(6):506–16.
[21] Tversky A, Kahneman D. Advances in prospect theory: cumulative representation of uncertainty. J Risk Uncertain 1992;5(4):297–323.
[22] Wakker P. Prospect theory: for risk and ambiguity. Cambridge ; New York: Cambridge University Press; 2010.
[23] Kahneman D, Tversky A. Prospect theory: an analysis of decision under risk. Econometrica 1979;47(2):263–91.
[24] Abdellaoui M. Parameter-free elicitation of utility and probability weighting functions. Manag Sci 2000;46(11):1497–512.
[25] Lattimore P, Baker J, Witte A. The influence of probability on risky choice: a parametric examination. J Econ Behav Organ 1992;17(3):377–400.
[26] Prelec D. The probability weighting function. Econometrica 1998;66(3):497–527.
[27] KNMI. Potential wind speed measurements. URL: http://www.knmi.nl/klimatologie/onderzoeksgegevens/potentiele_wind/; 2013.
[28] Gualtieri G, Secci S. Comparing methods to calculate atmospheric stability-dependent wind speed profiles: a case study on coastal location. Renew Energy 2011;36(8):2189–204.
[29] Twidell J, Weir A. Renewable energy resources. 2nd ed. London/New York: Taylor & Francis; 2006.
[30] Enercon. ENERCON wind energy converters product overview. URL: http://www.enercon.de/p/downloads/EN_Productoverview_0710.pdf; 2010.
[31] SenterNovem. Windmap of the netherlands at an altitude of 100 m. KEMA Nederland B.V; Jun. 2005. Technical report.
[32] Tenne T. Transparency of the electricity market. URL: http://energieinfo.tennet.org/; 2011.
[33] World Energy Council. Performance of generating plant: new metrics for Industry in transition. London: World Energy Council; 2010.
[34] TradeWind. Integrating wind: developing europe's power market for the large-scale integration of wind power; May 2009. Technical report.
[35] Holttinen H, Milligan M, Ela E, VTT Technical Research Centre of Finland, National Renewable Energy Laboratory (U.S.). Design and operation of power systems with large amounts of wind power: final report, IEA Wind Task 25, Phase One, 2006-2008. Espoo, Finland: VTT Technical Research Centre of Finland; 2009.
[36] European Wind Energy Association. Wind energy – the facts: a guide to the technology, economics and future of wind power. London; Sterling, VA: Earthscan; 2009.
[37] Ummels B. Wind integration: power system operation with large-scale wind power in liberalised environments. PhD thesis. Delft: Technische Universiteit Delft; Feb. 2009.